

Probing neutrino-antineutrino interactions from light gauge boson production in proto-neutron stars

Marina Cermeño Gavilán

Institute of Theoretical Physics (IFT UAM/CSIC)

Based on: Cerdeño, **Cermeño**, Farzan, PRD 107 (2023) 123012

September 12, 2023



CSIC

CONSEJO SUPERIOR DE INVESTIGACIONES CIENTÍFICAS



Instituto de
Física
Teórica
UAM-CSIC



EXCELENCIA
SEVERO
OCHOA

New light mediators in the neutrino (ν) sector



©D. G. Cerdeño

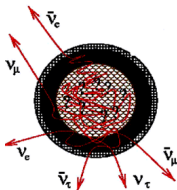
- Two of the most important challenges in cosmology and particle physics: understanding the dark matter nature and the lepton flavour violation in ν propagation
- Beyond the Standard Model realisations that feature **new low-mass mediators**
 - Well-motivated low-mass mediator models postulate the existence of new heavy gauge-singlet fermions that mix with the SM ν 's and can explain their lightness
 - Some models can explain the discrepancy in the muon anomalous magnetic moment, $(g - 2)_\mu$, and connect to a secluded sector that could account for the dark matter content in the Universe $\Rightarrow U(1)_{L_\mu - L_\tau}$ the simplest extension
 - Low-mass mediator scenarios provide new interactions in the neutrino sector

Supernova neutrinos

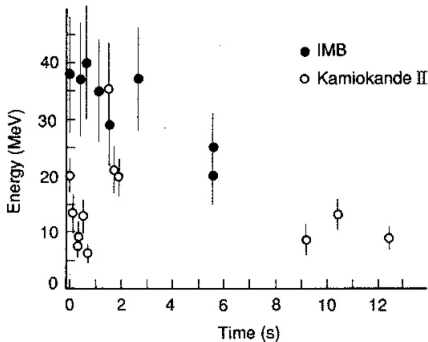
ν 's are crucial in proto-NS evolution \Rightarrow good sites to test new ν interactions

During the final phases of core collapse SN ν 's are copiously produced in the proto-NS interior ($n_\nu \sim 10^{36} \text{ cm}^{-3}$) and trapped due to their scattering with N s

After a second, they are emitted as the star cools down (Kelvin-Helmholtz cooling)

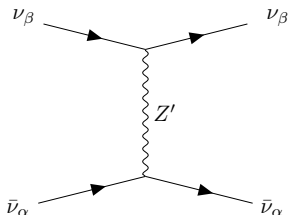
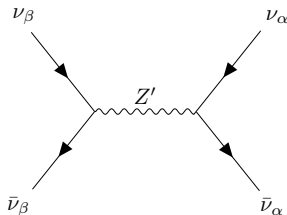


- Emitted ν 's observed during $t_{\text{signal}} \sim 10$ s from the SN 1987A
- t_{signal} proportional to the ν diffusion time in the stellar material $t_{\text{signal}} \sim 10 t_{\text{diff}}$
- The observed emission time is compatible with the one predicted by the SM



On-shell production of light mediators in the SN interior

Neutrino self-interactions take place in models featuring light mediators

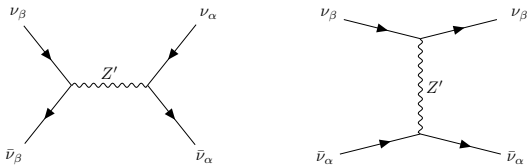


Z' can be **produced on-shell** via $\nu\bar{\nu}$ interactions **if $m_{Z'} \sim T \sim 30$ MeV**

We study the effect on the SN neutrino flux duration in two regimes

- Large coupling regime: $\nu - \bar{\nu}$ interaction rate, $\mathcal{R}_{\nu\bar{\nu}}$, larger than the $\nu - N$ one, $\mathcal{R}_{\nu N}$
- Small coupling regime: Z' decay length $\ell_{Z'} > 3$ m \sim standard ν mean free path

Neutrino-antineutrino coalescence in the $U(1)_{L_\mu-L_\tau}$ model



- The $U(1)_{L_\mu-L_\tau}$ model is a simple anomaly-free extension of the SM which features a Z' vector boson that mediates new interactions in the neutrino sector

$$\mathcal{L}_{L_\mu-L_\tau} = -\frac{1}{4}Z'^{\alpha\beta}Z'_{\alpha\beta} + \frac{m_{Z'}^2}{2}Z'_\alpha Z'^\alpha + Z'_\alpha g_{\mu-\tau} (\bar{\mu}\gamma^\alpha\mu + \bar{\nu}_\mu\gamma^\alpha P_L\nu_\mu - \bar{\tau}\gamma^\alpha\tau - \bar{\nu}_\tau\gamma^\alpha P_L\nu_\tau)$$

$Z'_{\alpha\beta} \equiv \partial_\alpha Z'_\beta - \partial_\beta Z'_\alpha$ the field strength tensor, $P_L = \frac{1}{2}(1 - \gamma_5)$ the left chirality projector

$\beta = \mu, \tau$: tree level coupling only to $\mu, \tau, \nu_\mu, \nu_\tau$ and their antiparticles

$m_{Z'}$ the mass of the gauge boson, $g_{\mu-\tau}$ the gauge coupling

Large coupling regime: Neutrino energy redistribution

- If $\mathcal{R}_{\nu\bar{\nu}} \gtrsim \mathcal{R}_{\nu N}$, ν 's will behave like tightly coupled perfect fluid and t_{diff} will not be affected
Dicus et al., PLB 218 (1989) 84
- Linear momentum conservation \Rightarrow short-ranged $\nu - \bar{\nu}$ interactions cannot change the energy flux of the $\nu + \bar{\nu}$ gas
- $\nu - \bar{\nu}$ **coalescence can redistribute ν and $\bar{\nu}$ energies** (narrower around $m_Z/2$) with a rate larger than that of ν scattering off the background matter
- **Less energetic ν will gain energy** and will become **more bounded to stellar matter** since $\sigma_{\nu N} \propto E_\nu^2 \Rightarrow$ **increase of t_{diff}**
- The fraction of ν_μ and ν_τ with $E_\nu < T$ is only 8% of the whole ν density, impact on t_{diff} not observable in the SN 1987A data \Rightarrow future SN detection?
- Effects on the neutrino energy flux and outflow checked in the recent papers *Fiorillo et al. (2023), arXiv: 2307.15115, 2307.15122* using relativistic hydrodynamics confirming too small differences to be distinguishable

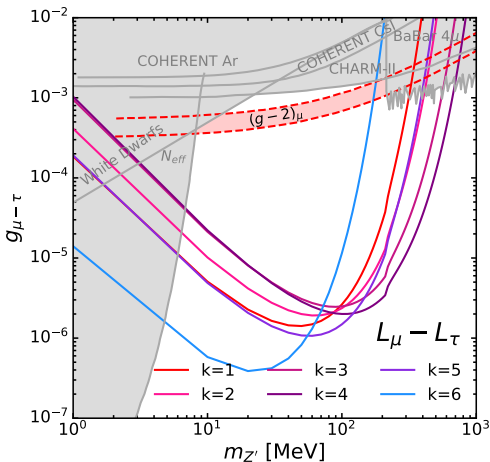
Large coupling regime: Neutrino energy redistribution

Values of $(g_{\mu-\tau}, m_{Z'})$ for which the average of the $\nu\bar{\nu}$ scattering rate via Z' equals the SM value in each of the proto-NS shells \Rightarrow neutrino energy redistribution for $\sim 10\%$ of the total neutrinos emitted

Cerdeño, **Cermeño**, Farzan, *arXiv: 2301.00661*

T and n_B from Fischer et al., *PRD 85 (2012) 083003*

	R (km)	T (MeV)	n_B (fm^{-3})
$k=1$	5.0	15	0.5
$k=2$	7.5	20	0.3
$k=3$	10.0	28	0.15
$k=4$	15.0	33	0.06
$k=5$	17.5	18	0.03
$k=6$	20.0	7	0.008



Small coupling regime: Shortening of the ν flux duration

- We study cases where $3 \text{ m} < \ell_{Z'} < 20 \text{ km}$
- For $\ell_{Z'} > R_{ns} \sim 20 \text{ km}$, t_{signal} can be shortened by half if the energy carried away by the Z' per unit time $\gtrsim 3 \times 10^{52} \text{ erg/s}$ *Burrows, Turner, Brinkmann, PRD 39 (1989) 1020, Choi, Santamaria, PRD 42 (1990) 293, Raffelt, Phys. Rept. 198 (1990) 1*
- In a time $\tau_{\nu\bar{\nu}\rightarrow Z'} = c/\langle\mathcal{R}_{\nu\bar{\nu}\rightarrow Z'}\rangle$, $\nu\bar{\nu} \rightarrow Z'$ and Z' decay into $\nu\bar{\nu}$ at a distance $\ell_{Z'}$ $\langle\mathcal{R}_{\nu\bar{\nu}\rightarrow Z'}\rangle$ the average in E_ν of the $\nu\bar{\nu} \rightarrow Z'$ interaction rate
- After time t , $\nu\bar{\nu}$ pairs take $N = t/\tau_{\nu\bar{\nu}\rightarrow Z'}$ random steps, which takes them on average a distance $\sqrt{N}\ell_{Z'}$ far away from where they started

For $\sqrt{N}\ell_{Z'} = R_{ns} \Rightarrow$ the ν diffusion time $t_{\text{diff}}^{\text{new}} = (R_{ns}/\ell_{Z'})^2 \tau_{\nu\bar{\nu}\rightarrow Z'}$

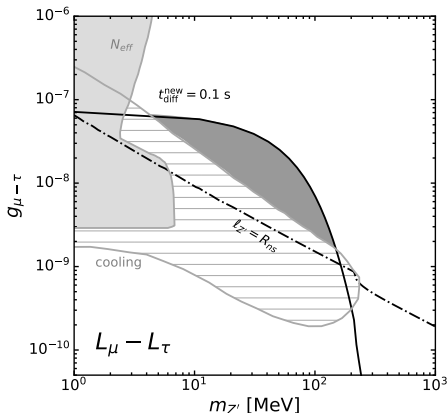
Describing the proto-NS interior with 6 different shells of radius R_k (different T)

$$t_{\text{diff}}^{\text{new}} = \sum_{k=1}^n \frac{(R_k^2 - R_{k-1}^2)}{(\ell_{Z'}^k)^2} \tau_{\nu\bar{\nu}\rightarrow Z'}^k$$

Small coupling regime: Bounds $U(1)_{L_\mu-L_\tau}$

The total energy in form of $\nu_{\mu,\tau}, \bar{\nu}_{\mu,\tau}$ at the on-set of the cooling phase is $\sim 3 \times 10^{51}$ erg

- If $t_{\text{diff}}^{\text{new}} \leq 0.1$ s, the energy transfer via the Z' production will be comparable to the luminosity within the SM, t_{signal} **shortened by half** \Rightarrow lower limit as long as $l_{Z'} < R_{\text{ns}}$
Cerdeño, Cermeño, Farzan, arXiv: 2301.00661



Cooling bounds from *Croon et al., JHEP 01 (2021) 107* (t_{signal} shortened by half when Z' decays outside the proto-NS)

Conclusions

- We have investigated the effect of the on-shell production of low-mass vector mediators Z' by $\nu\bar{\nu}$ interactions in the core of proto-NS on the SN ν signal duration
- If $\nu\bar{\nu}$ interaction rate via Z' exceeds the $\nu - N$ one, ν energies can be redistributed \Rightarrow enhancement in the burst duration. Small effect to impact the SN 1987A data
- On the region of the parameter space where the decay length of Z' is larger than the standard ν mean free path but small enough so that the Z' decays inside the proto-NS, the ν burst duration can be significantly reduced
- Based on the previous, we extend cooling bounds for the $U(1)_{L_\mu-L_\tau}$ parameter space ruling out couplings up to $\sim 6 \times 10^{-8}$

Backup slides

Proto-NS birth

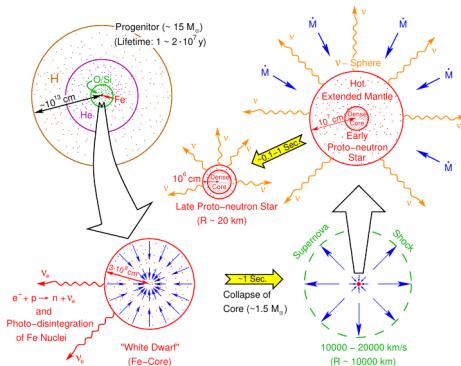


Fig. 2 Evolution of a massive star from the onset of iron-core collapse to a neutron star. The progenitor has developed a typical onion-shell structure with layers of increasingly heavier elements surrounding the iron core at the center (upper left corner). Like a white dwarf star, this iron core (enlarged on the lower left side) is stabilized mostly by the fermion pressure of nearly degenerate electrons. It becomes gravitationally unstable when the rising temperatures begin to allow for partial photo-disintegration of iron-group nuclei to α -particles and nucleons. The contraction accelerates to a dynamical collapse by electron captures on bound and free protons, releasing electron neutrinos (ν_e), which initially escape freely. Only fractions of a second later, the catastrophic infall is stopped because nuclear-matter density is reached and a proto-neutron star begins to form. This gives rise to a strong shock wave which travels outward and disrupts the star in a supernova explosion (lower right). The nascent neutron star is initially very extended (enlarged in the upper right corner), and contracts to a more compact object while accreting more matter (visualized by the mass-accretion rate \dot{M}) within the first second of its evolution. This phase as well as the subsequent cooling and neutronization of the compact remnant are driven by the emission of neutrinos and antineutrinos of all flavors (indicated by the symbol ν), which diffuse out from the dense and hot super-nuclear core over tens of seconds. (Figure adapted from [Burrows, 1990b](#))

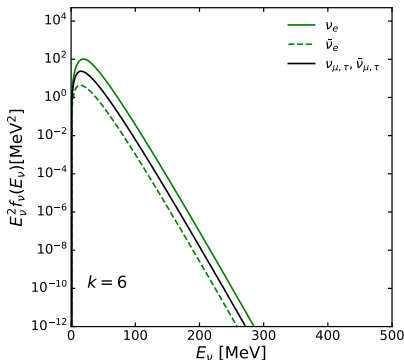
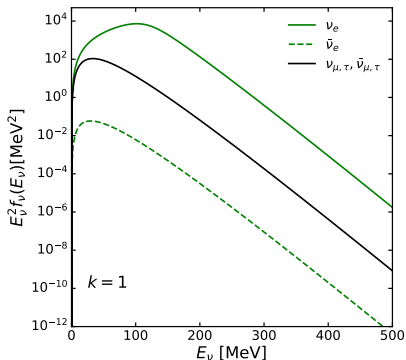
Neutrino energy distribution inside the proto-NS

T , n_B and Y_e from Fischer et al., PRD 85 (2012) 083003,

μ_n^* , μ_p^* , $\mu_{\nu_e}^*$ and m_N^* from Cerdeño, Cermeño, Pérez-García and Reid, PRD 104 (2021) 063013

Neutrino's chemical potentials for the different flavour $\mu_{\bar{\nu}_e}^* = -\mu_{\nu_e}^*$, $\langle E_{\nu_e} \rangle = (3/4)\mu_{\nu_e}^*$, $\mu_{\nu_{\mu,\tau}} = \mu_{\bar{\nu}_{\mu,\tau}} = 0$, $\langle E_{\nu_{\mu,\tau}} \rangle = \pi T$

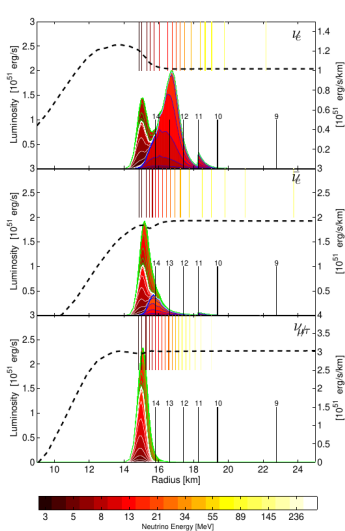
	R (km)	T (MeV)	n_B (fm $^{-3}$)	Y_e	μ_n^* (MeV)	μ_p^* (MeV)	$\mu_{\nu_e}^*$ (MeV)	m_N^* (MeV)
$k = 1$	5.0	15	0.5	0.3	496.6	405.4	114.6	249.6
$k = 2$	7.5	20	0.3	0.28	530.0	458.3	102.7	384.9
$k = 3$	10.0	28	0.15	0.25	656.5	601.9	79.9	599.4
$k = 4$	15.0	33	0.06	0.2	779.8	723.0	29.0	786.0
$k = 5$	17.5	18	0.03	0.1	858.7	813.1	14.4	857.0
$k = 6$	20.0	7	0.008	0.05	917.2	893.9	12.5	915.9



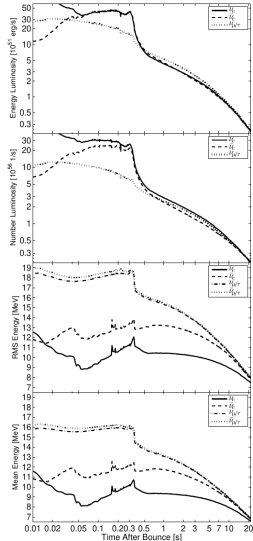
Neutrino luminosity

Fischer et al., PRD 85 (2012) 083003

$$M_{\text{proj}} = 18 M_{\odot}$$



(a) 5 seconds post bounce



Relevant interactions inside SN

Janka arXiv: 1702.08713. In 'Handbook of Supernovae,' Springer

Table 1 Most important neutrino processes in supernova and proto-neutron star matter.

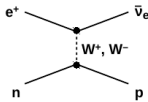
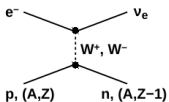
Process	Reaction ^a
Beta-processes (direct URCA processes)	
electron and ν_e absorption by nuclei	$e^- + (A, Z) \longleftrightarrow (A, Z-1) + \nu_e$
electron and ν_e captures by nucleons	$e^- + p \longleftrightarrow n + \nu_e$
positron and $\bar{\nu}_e$ captures by nucleons	$e^+ + n \longleftrightarrow p + \bar{\nu}_e$
“Thermal” pair production and annihilation processes	
Nucleon-nucleon bremsstrahlung	$N + N \longleftrightarrow N + N + \nu + \bar{\nu}$
Electron-positron pair process	$e^- + e^+ \longleftrightarrow \nu + \bar{\nu}$
Plasmon pair-neutrino process	$\tilde{\gamma} \longleftrightarrow \nu + \bar{\nu}$
Reactions between neutrinos	
Neutrino-pair annihilation	$\nu_e + \bar{\nu}_e \longleftrightarrow \nu_x + \bar{\nu}_x$
Neutrino scattering	$\nu_x + \{\nu_e, \bar{\nu}_e\} \longleftrightarrow \nu_x + \{\nu_e, \bar{\nu}_e\}$
Scattering processes with medium particles	
Neutrino scattering with nuclei	$\nu + (A, Z) \longleftrightarrow \nu + (A, Z)$
Neutrino scattering with nucleons	$\nu + N \longleftrightarrow \nu + N$
Neutrino scattering with electrons and positrons	$\nu + e^\pm \longleftrightarrow \nu + e^\pm$

^a N means nucleons, i.e., either n or p , $\nu \in \{\nu_e, \bar{\nu}_e, \nu_\mu, \bar{\nu}_\mu, \nu_\tau, \bar{\nu}_\tau\}$, $\nu_x \in \{\nu_\mu, \bar{\nu}_\mu, \nu_\tau, \bar{\nu}_\tau\}$

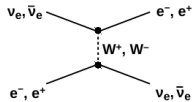
Relevant interactions inside SN

Janka arXiv: 1702.08713. In 'Handbook of Supernovae,' Springer

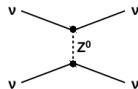
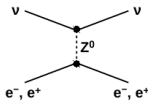
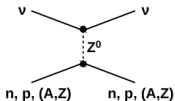
CC β -processes



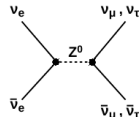
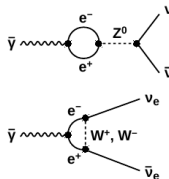
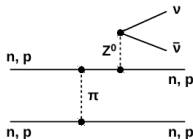
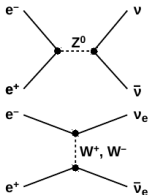
CC scattering process



NC scattering processes ($\nu = \nu_e, \bar{\nu}_e, \nu_\mu, \bar{\nu}_\mu, \nu_\tau, \bar{\nu}_\tau$)



Neutrino-pair ("thermal") processes



Neutrino decoupling SM

Janka arXiv: 1702.08713. In 'Handbook of Supernovae,' Springer

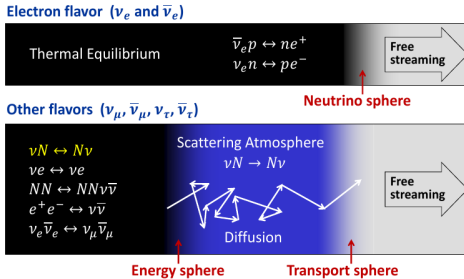


Fig. 4 Sketch of the transport properties of electron-flavor neutrinos and antineutrinos (*upper part*) compared to heavy-lepton neutrinos (*lower part*). In the supernova core ν_e and $\bar{\nu}_e$ interact with the stellar medium by charged-current absorption and emission reactions, which provide a major contribution to their opacities and lead to a strong energetic coupling up to the location of their neutrinospheres, outside of which both chemical equilibrium between neutrinos and stellar matter (indicated by the black region) and diffusion cannot be maintained. In contrast, heavy-lepton neutrinos are energetically less tightly coupled to the stellar plasma, mainly by pair creation reactions like nucleon bremsstrahlung, electron-positron annihilation and $\nu_e \bar{\nu}_e$ annihilation. The total opacity, however, is determined mostly by neutrino-nucleon scatterings, whose small energy exchange per scattering does not allow for an efficient energetic coupling. Therefore heavy-lepton neutrinos fall out of thermal equilibrium at an energy sphere that is considerably deeper inside the nascent neutron star than the transport sphere, where the transition from diffusion to free streaming sets in. The blue band indicates the scattering atmosphere where the heavy-lepton neutrinos still collide frequently with neutron and protons and lose some of their energy, but cannot reach equilibrium with the background medium any longer. (Figure adapted from [Raffelt 2012](#), courtesy of Georg Raffelt)

SN phases

Janka arXiv: 1702.08713. In 'Handbook of Supernovae,' Springer

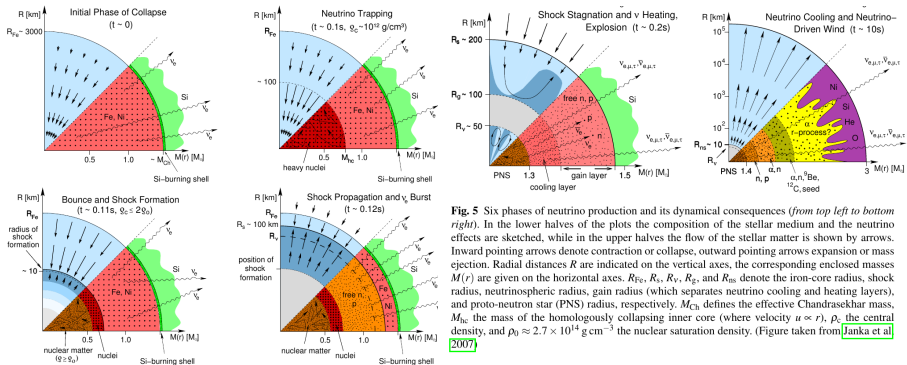


Fig. 5 Six phases of neutrino production and its dynamical consequences (from top left to bottom right). In the lower halves of the plots the composition of the stellar medium and the neutrino effects are sketched, while in the upper halves the flow of the stellar matter is shown by arrows. Inward pointing arrows denote contraction or collapse, outward pointing arrows expansion or mass ejection. Radial distances R are indicated on the vertical axes, the corresponding enclosed masses $M(r)$ are given on the horizontal axes. R_{Fe} , R_s , R_v , R_g , and R_{ns} denote the iron-core radius, shock radius, neutrinospheric radius, gain radius (which separates neutrino cooling and heating layers), and proto-neutron star (PNS) radius, respectively. M_{Ch} defines the effective Chandrasekhar mass, M_{hc} the mass of the homologously collapsing inner core (where velocity $u \propto r$), ρ_c the central density, and $\rho_0 \approx 2.7 \times 10^{14} \text{ g cm}^{-3}$ the nuclear saturation density. (Figure taken from Janka et al 2007)

Effective nucleon masses and chemical potentials

Considering the TM1 model for a $18 M_{\odot}$ progenitor in a relativistic mean field approach:

- The baryonic density, n_B , temperature, T , and electron fraction, Y_e , derived by *Fischer et al.*, *PRD 85 (2012) 083003*
- The effective nucleon masses, m_N^* , and the neutrino and nucleon effective chemical potentials, $\mu_{\nu_e}^*$, μ_n^* , μ_p^* obtained by *Cerdeño, Cermeño, Pérez-García and Reid*, *PRD 104 (2021) 063013*
- $\mu_{\nu_e}^*$ is obtained solving the equilibrium equation that involves effective meson fields:
 $\mu_n^* + \mu_{\nu_e}^* = \mu_p^* + \mu_e^* + 2g_{\rho}\langle\rho\rangle$, where ρ is an effective field responsible of the strong interaction

	R (km)	T (MeV)	n_B (fm $^{-3}$)	Y_e	μ_n^* (MeV)	μ_p^* (MeV)	$\mu_{\nu_e}^*$ (MeV)	m_N^* (MeV)
$k = 1$	5.0	15	0.5	0.3	496.6	405.4	114.6	249.6
$k = 2$	7.5	20	0.3	0.28	530.0	458.3	102.7	384.9
$k = 3$	10.0	28	0.15	0.25	656.5	601.9	79.9	599.4
$k = 4$	15.0	33	0.06	0.2	779.8	723.0	29.0	786.0
$k = 5$	17.5	18	0.03	0.1	858.7	813.1	14.4	857.0
$k = 6$	20.0	7	0.008	0.05	917.2	893.9	12.5	915.9

TABLE I. Values of neutron effective chemical potential, μ_n^* , proton effective chemical potential, μ_p^* , electron neutrino effective chemical potential, $\mu_{\nu_e}^*$, and nucleon effective mass, m_N^* , for the spherical shells (labeled by the index k and defined by an outer radius R) that we consider at 1 s after bounce, with a baryonic density, n_B , temperature, T and electron fraction, Y_e . Temperatures, densities and electron fraction are taken from Ref. [45].

Effective nucleon masses and chemical potentials

The equation of state of nuclear matter is constructed using the relativistic mean field (RMF) theory with the TM1 parameter set *Sugahara and H. Toki, Nucl. Phys. A 579 (1994) 557, Shen et al., Nucl. Phys. A 637 (1998) 435*

- In the RMF approach baryons are considered Dirac quasiparticles moving in classical meson fields and the field operators, ϕ , are replaced by their expectation values, $\langle\phi\rangle$
- The TM1 model is a representative example where the set of parameters used can smoothly connect low and high density regions in the dynamical stellar description
- The presence of an effective nucleon mass and effective chemical potential is due to the non vanishing values of the Lorentz scalar meson, $\langle\sigma\rangle$, Lorentz vector, $\langle\omega_\mu\rangle$, and vector-isovector, $\langle\vec{\rho}_\mu\rangle$, meson fields

The effective nucleon mass $m_N^* = m_N - g_{\sigma N}\langle\sigma\rangle$

Effective nucleon chemical potentials, $\mu_i^* = \mu_i - g_{\omega N}\langle\omega\rangle - g_{\rho N}t_{3i}\langle\rho\rangle$ ($i = n, p$)

$g_{\sigma N}$, $g_{\omega N}$, and $g_{\rho N}$ are dimensionless constants that couple nucleons to the σ , ω , and ρ mesons t_{3i} is the third component of the isospin of the proton or the neutron, $i = p, n$

This parameter set includes self-interaction terms from scalar, vector and vector-isovector mesons in non isospin symmetric nuclear matter at finite temperature

TM1 interaction terms are constrained by the nuclear masses, radii, neutron skins and their excitations

When applied to the derived proto-NS, the mass-radius diagram allows to fulfil the subsequent two solar mass constraint from recent observations of older objects.

Relativistic mean field theory lagrangian

The relativistic mean field theory lagrangian

Sugahara and H. Toki, Nucl. Phys. A 579 (1994) 557, Shen et al., Nucl. Phys. A 637 (1998) 435

$$\begin{aligned}\mathcal{L}_{RMF} = & \bar{\psi} \left[i\gamma_{\mu} \partial^{\mu} - M - g_{\sigma} \sigma - g_{\omega} \gamma_{\mu} \omega^{\mu} - g_{\rho} \gamma_{\mu} \tau_a \rho^{a\mu} - e\gamma_{\mu} \frac{1 - \tau_3}{2} A^{\mu} \right] \psi \\ & + \frac{1}{2} \partial_{\mu} \sigma \partial^{\mu} \sigma - \frac{1}{2} m_{\sigma}^2 \sigma^2 - \frac{1}{3} g_2 \sigma^3 - \frac{1}{4} g_3 \sigma^4 \\ & - \frac{1}{4} W_{\mu\nu} W^{\mu\nu} + \frac{1}{2} m_{\omega}^2 \omega_{\mu} \omega^{\mu} + \frac{1}{4} c_3 (\omega_{\mu} \omega^{\mu})^2 \\ & - \frac{1}{4} R_{\mu\nu}^a R^{a\mu\nu} + \frac{1}{2} m_{\rho}^2 \rho_{\mu}^a \rho^{a\mu} - \frac{1}{4} F_{\mu\nu} F^{\mu\nu},\end{aligned}$$

where

$$\begin{aligned}W^{\mu\nu} &= \partial^{\mu} \omega^{\nu} - \partial^{\nu} \omega^{\mu}, \\ R^{a\mu\nu} &= \partial^{\mu} \rho^{a\nu} - \partial^{\nu} \rho^{a\mu} + g_{\rho} \epsilon^{abc} \rho^{b\mu} \rho^{c\nu}, \\ F^{\mu\nu} &= \partial^{\mu} A^{\nu} - \partial^{\nu} A^{\mu}.\end{aligned}$$

The nucleon field ψ having the mass M interacts with σ , ω_{μ} and ρ_{μ}^a mesons and the photon field A_{μ} .

Self-coupling terms with the coupling constants g_2 and g_3 for the σ meson and with the coupling constant c_3 for the ω meson

The coupling strengths, g 's, and the meson masses, m 's, are the parameters of this theory.

Different parameter sets for the Lagrangian

Sugahara and H. Toki, Nucl. Phys. A 579 (1994) 557

Table 2

The parameters of the lagrangian determined by the least-squares fitting procedure are listed under TM1 for the heavy nuclei and TM2 for the light nuclei. For comparison, the parameters of NL1 and NL-SH are also listed under the column of NL1 and NL-SH, respectively

	TM1	TM2	NL1	NL-SH
M (MeV)	938.0	938.0	938.0	939.0
m_σ (MeV)	511.198	526.443	492.250	526.059
m_ω (MeV)	783.0	783.0	795.359	783.0
m_ρ (MeV)	770.0	770.0	763.0	763.0
g_σ	10.0289	11.4694	10.1377	10.444
g_ω	12.6139	14.6377	13.2846	12.945
g_ρ	4.6322	4.6783	4.9757	4.383
g_2 (fm ⁻¹)	-7.2325	-4.4440	-12.1724	-6.9099
g_3	0.6183	4.6076	-36.2646	-15.8337
c_3	71.3075	84.5318	0.0	0.0

Relation between ν emission time and diffusion time

- At the onset of the cooling phase (~ 1 s after the bounce), the luminosity is of the order of 10^{52} erg s^{-1} for each ν and $\bar{\nu}$ species
- The outer layers cool down fast, the neutrinosphere recedes to smaller radii and the luminosity quickly drops
- The neutrino emission is backed up with the diffusion of ν 's from the inner layers. Due to multiple scattering, ν 's take a sizable time to reach the outer layers of the proto-NS, from where they are radiated out with a time scale of
Janka arXiv: 1702.08713. In 'Handbook of Supernovae,' Springer

$$t_{\text{signal}} \sim \frac{3}{\pi^2} \frac{E_{th}^{tot}}{2E_{th}^{\nu}} R_{ns}^2 \left\langle \frac{1}{\lambda} \right\rangle \sim 10 \text{ s},$$

- E_{th}^{tot} and E_{th}^{ν} are the total baryon and neutrino thermal energies, $E_{th}^{tot}/(2E_{th}^{\nu}) \sim 10$
- $\langle 1/\lambda \rangle$ the average of the inverse of the neutrino mean free path
- $R_{ns}^2 \langle 1/\lambda \rangle$ (where R_{ns} is the radius of the neutrinosphere) gives the time scale of the diffusion of a single particle with a velocity of light and with random walk steps of λ
- In order to fulfill $t_{\text{signal}} \sim 10$ s, $R_{ns}^2 \langle 1/\lambda \rangle \sim 3$ s/c. From our calculation we get $R_{ns}^2 \langle 1/\lambda \rangle \sim 2.9$ s/c for electron neutrinos and 1.3 s/c for muon and tau neutrinos

Calculation of the mean free path

The average of the inverse of the mean free path for neutrino scattering on a target particle, j , can be calculated by integrating the invariant cross section, $\sigma_{\nu\beta,j}$, as follows

$$\langle 1/\lambda_{\nu\beta} \rangle = \frac{\int dE_{\nu\beta} f(E_{\nu\beta}, \mu_{\nu\beta}^*, T) E_{\nu\beta}^2 \lambda_{\nu\beta}^{-1}(E_{\nu\beta})}{\int dE_{\nu\beta} f(E_{\nu\beta}, \mu_{\nu\beta}^*, T) E_{\nu\beta}^2},$$

where $\beta = e, \mu, \tau$ indicates the neutrino flavour and

$$\lambda_{\nu\beta}^{-1}(E_{\nu\beta}) = \sum_j \int g_j \frac{d^3 \vec{p}_j}{(2\pi)^3} f(E_j, \mu_j^*, T) |v_{\nu\beta}^{\vec{}} - \vec{v}_j| \sigma_{\nu\beta,j}$$

is the inverse of the neutrino mean free path including neutrino scattering with all possible targets. g_j denotes the relativistic degrees of freedom of the corresponding target and $|v_{\nu\beta}^{\vec{}} - \vec{v}_j|$ is the relative velocity between the neutrino and the target, and $f(E, \mu^*, T)$ are the Fermi-Dirac distribution functions. For a general 2 by 2 process,

$$|v_{\nu\beta}^{\vec{}} - \vec{v}_j| \sigma_{\nu\beta,j} = \int \frac{d^3 \vec{p}'_{\nu\beta}}{(2\pi)^3 2E'_{\nu\beta}} \int \frac{d^3 \vec{p}'_j}{(2\pi)^3 2E'_j} (2\pi)^4 \delta^{(4)}(p_{\nu\beta} + p_j - p'_{\nu\beta} - p'_j) \frac{|\overline{\mathcal{M}}|_{\nu\beta,j}^2}{4E_{\nu\beta} E_j} (1 - f(E'_{\nu\beta}, \mu_{\nu\beta}^*, T)) (1 - f(E'_j, \mu_j^*, T)),$$

where $E_{\nu\beta}$, E_j , $\vec{p}_{\nu\beta}$, \vec{p}_j are the energies and momenta of the incoming particles, $E'_{\nu\beta}$, E'_j , $\vec{p}'_{\nu\beta}$, \vec{p}'_j are those of the outgoing states, and $p_{\nu\beta}$, p_j , $p'_{\nu\beta}$, p'_j are the corresponding four-momenta.

Large coupling regime: Neutrino energy redistribution

- Linear momentum conservation \Rightarrow short-ranged $\nu - \bar{\nu}$ interactions inside the proto-NS cannot change the energy flux of $\nu - \bar{\nu}$ gas
- $\nu - \bar{\nu}$ **coalescence can redistribute ν and $\bar{\nu}$ energies** with a rate larger than that of scattering off the background matter

ν with energy $E_1 = \pi T - \Delta$ interacting with $\bar{\nu}$ with energy $E_2 = \frac{m_{Z'}^2}{2E_1(1-\cos\theta)} > E_1$ produce the Z' on-shell (Δ positive constant and θ the angle between ν and $\bar{\nu}$)

The final ν and $\bar{\nu}$ from the Z' decay will have a flat energy distribution in the range

$$[(E_1 + E_2)(1 - v_{Z'})/2, (E_1 + E_2)(1 + v_{Z'})/2],$$

with $v_{Z'} = (1 - m_{Z'}^2/(E_1 + E_2)^2)^{1/2}$

The less energetic ν with initial energy E_1 will gain energy and will become more bounded to stellar matter ($\sigma_{\nu,N} \propto E_\nu^2$)

- The fraction of ν_μ and ν_τ with $E_\nu < T$ ($E_\nu < T/3$) is only 8% (0.48%) of the whole number density, impact on t_{diff} not observable in the SN 1987A data
- Future SN detection?

Calculation of the $\nu - \bar{\nu}$ scattering rate via Z'

The average of the neutrino-antineutrino scattering rate

$$\langle \mathcal{R}_{\nu_\beta \bar{\nu}_\beta \rightarrow Z' \rightarrow \nu_\alpha \bar{\nu}_\alpha} \rangle = \frac{\int dE_{\nu_\beta} f(E_{\nu_\beta}, \mu_{\nu_\beta}^*, T) E_{\nu_\beta}^2 \mathcal{R}_{\nu_\beta \bar{\nu}_\beta \rightarrow Z' \rightarrow \nu_\alpha \bar{\nu}_\alpha}(E_{\nu_\beta})}{\int dE_{\nu_\beta} f(E_{\nu_\beta}, \mu_{\nu_\beta}^*, T) E_{\nu_\beta}^2}$$

where $\beta = e, \mu, \tau$ indicates the neutrino flavour and

$$\mathcal{R}_{\nu_\beta \bar{\nu}_\beta \rightarrow Z' \rightarrow \nu_\alpha \bar{\nu}_\alpha}(E_{\nu_\beta}) = \int \frac{d^3 \vec{p}_{\bar{\nu}_\beta}}{(2\pi)^3} f(E_{\bar{\nu}_\beta}, \mu_{\bar{\nu}_\beta}^*, T) |\vec{v}_{\nu_\beta} - \vec{v}_{\bar{\nu}_\beta}| \sigma_{\nu_\beta, \bar{\nu}_\beta}$$

is the neutrino-antineutrino scattering rate via Z' , $|\vec{v}_{\nu_\beta} - \vec{v}_{\bar{\nu}_\beta}|$ is the relative velocity between neutrinos and antineutrinos and $\sigma_{\nu_\beta, \bar{\nu}_\beta}$ is the neutrino-antineutrino scattering cross section, its product

$$|\vec{v}_{\nu_\beta} - \vec{v}_{\bar{\nu}_\beta}| \sigma_{\nu_\beta, \bar{\nu}_\beta} = \int \frac{d^3 \vec{p}'_{\nu_\alpha}}{(2\pi)^3 2E'_{\nu_\alpha}} \int \frac{d^3 \vec{p}'_{\bar{\nu}_\alpha}}{(2\pi)^3 2E'_{\bar{\nu}_\alpha}} (2\pi)^4 \delta^{(4)}(p_{\nu_\beta} + p_{\bar{\nu}_\beta} - p'_{\nu_\alpha} + p'_{\bar{\nu}_\alpha}) \frac{|\overline{\mathcal{M}}|_{\nu_\beta, \bar{\nu}_\beta}^2}{4E_{\nu_\beta} E_{\bar{\nu}_\beta}} \mathcal{F}(E'_{\nu_\alpha}, E'_{\bar{\nu}_\alpha})$$

with $E_{\nu_\beta}, E_{\bar{\nu}_\beta}, \vec{p}_{\nu_\beta}, \vec{p}_{\bar{\nu}_\beta}$ the energies and momenta of the incoming particles, $E'_{\nu_\alpha}, E'_{\bar{\nu}_\alpha}, \vec{p}'_{\nu_\alpha}, \vec{p}'_{\bar{\nu}_\alpha}$ those of the outgoing states, and $p_{\nu_\beta}, p_{\bar{\nu}_\beta}, p'_{\nu_\alpha}, p'_{\bar{\nu}_\alpha}$ the corresponding four-momenta

$\mathcal{F}(E'_{\nu_\alpha}, E'_{\bar{\nu}_\alpha}) = (1 - f(E'_{\nu_\alpha}, \mu_{\nu_\alpha}^*, T))(1 - f(E'_{\bar{\nu}_\alpha}, \mu_{\bar{\nu}_\alpha}^*, T))$ accounts for Pauli blocking in the outgoing states

Narrow Width Approximation

In the parameter space under analysis

- The resonant production of the Z' boson is the leading new physics process
- $\Gamma_{Z' \rightarrow \bar{\nu}_\beta \nu_\beta} / m_{Z'} \ll 1$ is fulfilled, with $\Gamma_{Z' \rightarrow \bar{\nu}_\beta \nu_\beta}$ the decay width of the Z' into neutrinos
- The narrow width approximation can be used to obtain the neutrino-antineutrino scattering rate

$$\mathcal{R}_{\nu_\beta \bar{\nu}_\beta \rightarrow Z' \rightarrow \nu_\alpha \bar{\nu}_\alpha}(E_{\nu_\beta}) = \frac{1}{32\pi} \int_{E_{\bar{\nu}_\beta}^{\min}}^{\infty} dE_{\bar{\nu}_\beta} \frac{f(E_{\bar{\nu}_\beta}, \mu_{\bar{\nu}_\beta}^*, T) E_{\bar{\nu}_\beta}}{E_{\bar{\nu}_\beta} + E_{\nu_\beta}} \left(\frac{m_{Z'}}{E_{\bar{\nu}_\beta} E_{\nu_\beta}} \right)^2 |\overline{\mathcal{M}}|_{\nu_\beta \bar{\nu}_\beta \rightarrow Z'}^2 \frac{\Gamma_{Z' \rightarrow \nu_\alpha \bar{\nu}_\alpha}}{\Gamma_{Z'}^{\text{tot}}},$$

- $E_{\bar{\nu}_\beta}^{\min} = m_{Z'}^2 / (4E_{\nu_\beta})$
- The total Z' decay width $\Gamma_{Z'}^{\text{tot}} = \sum_\beta \Gamma_{Z' \rightarrow \bar{\nu}_\beta \nu_\beta} + \Gamma_{Z' \rightarrow \beta^+ \beta^-}$, where $\beta = \mu, \tau$
- The average of the $\nu - \bar{\nu}$ scattering rate

$$\langle \mathcal{R}_{\nu_\beta \bar{\nu}_\beta \rightarrow Z' \rightarrow \nu_\alpha \bar{\nu}_\alpha} \rangle = \frac{\int dE_{\nu_\beta} f(E_{\nu_\beta}, \mu_{\nu_\beta}^*, T) E_{\nu_\beta}^2 \mathcal{R}_{\nu_\beta \bar{\nu}_\beta \rightarrow Z' \rightarrow \nu_\alpha \bar{\nu}_\alpha}(E_{\nu_\beta})}{\int dE_{\nu_\beta} f(E_{\nu_\beta}, \mu_{\nu_\beta}^*, T) E_{\nu_\beta}^2}$$

$\nu - \bar{\nu}$ coalescence rate and Z' decay length

The rate of the scattering of a single ν off any $\bar{\nu}$ in the medium producing the Z' on-shell can be computed via the following relation,

$$\mathcal{R}_{\nu\bar{\nu}\rightarrow Z'}(E_{\nu\beta}) = \frac{1}{32\pi} \int_{E_{\bar{\nu}\beta}^{\min}}^{\infty} dE_{\bar{\nu}\beta} \frac{f(E_{\bar{\nu}\beta}, \mu_{\bar{\nu}\beta}^*, T) E_{\bar{\nu}\beta}}{E_{\bar{\nu}\beta} + E_{\nu\beta}} \left(\frac{m_{Z'}}{E_{\bar{\nu}\beta} E_{\nu\beta}} \right)^2 |\overline{\mathcal{M}}|_{\nu\bar{\nu}\rightarrow Z'}^2.$$

The time scale of the interaction can be defined as $\tau_{\nu\bar{\nu}\rightarrow Z'} = c / \langle \mathcal{R}_{\nu\bar{\nu}\rightarrow Z'} \rangle$, with

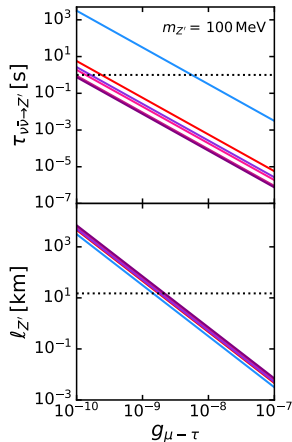
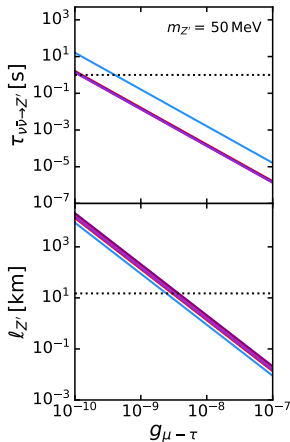
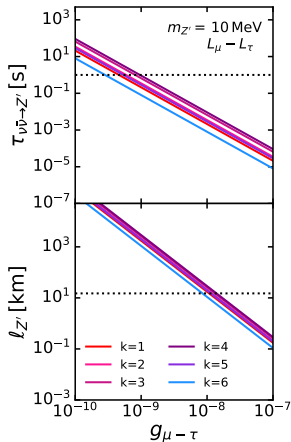
$$\langle \mathcal{R}_{\nu\bar{\nu}\rightarrow Z'} \rangle = \frac{\int dE_{\nu\beta} f(E_{\nu\beta}, \mu_{\nu\beta}^*, T) E_{\nu\beta}^2 \mathcal{R}_{\nu\bar{\nu}\rightarrow Z'}(E_{\nu\beta})}{\int dE_{\nu\beta} f(E_{\nu\beta}, \mu_{\nu\beta}^*, T) E_{\nu\beta}^2}.$$

The Z' decay length

$$\ell_{Z'} = \frac{\int \frac{d^3\vec{p}_{\nu\beta}}{(2\pi)^3} f(E_{\nu\beta}, \mu_{\nu\beta}^*, T) \int \frac{d^3\vec{p}_{\bar{\nu}\beta}}{(2\pi)^3} f(E_{\bar{\nu}\beta}, \mu_{\bar{\nu}\beta}^*, T) \sigma_{\nu\bar{\nu}\rightarrow Z'} |v_{\nu\beta}^{\rightarrow} - v_{\bar{\nu}\beta}^{\rightarrow}| \gamma_{Z'} v_{Z'} \frac{\hbar}{\Gamma_{Z'}^{\text{tot}}}}{\int \frac{d^3\vec{p}_{\nu\beta}}{(2\pi)^3} f(E_{\nu\beta}, \mu_{\nu\beta}^*, T) \int \frac{d^3\vec{p}_{\bar{\nu}\beta}}{(2\pi)^3} f(E_{\bar{\nu}\beta}, \mu_{\bar{\nu}\beta}^*, T) \sigma_{\nu\bar{\nu}\rightarrow Z'} |v_{\nu\beta}^{\rightarrow} - v_{\bar{\nu}\beta}^{\rightarrow}|},$$

where $v_{Z'}$ is the Z' velocity, $\gamma_{Z'} = E_{Z'}/m_{Z'}$ and $\sigma_{\nu\bar{\nu}\rightarrow Z'}$ is the cross section for $\nu\bar{\nu}$ coalescence

$\nu - \bar{\nu}$ coalescence rate and Z' decay length



Small coupling regime: Shortening of the ν flux duration

- We study cases when the Z' decay length, $\ell_{Z'}$, is **3 m** < $\ell_{Z'}$ < **20 km**

$\ell_{Z'}$ calculated multiplying the Z' lifetime by $\gamma_{Z'} = E_{Z'}/m_{Z'}$ and $v'_{Z'}$, averaged over $E_{Z'}$

$\langle \mathcal{R}_{\nu\bar{\nu}\rightarrow Z'} \rangle$ is the average in E_ν of the $\nu\bar{\nu} \rightarrow Z'$ interaction rate

$$\mathcal{R}_{\nu\bar{\nu}\rightarrow Z'}(E_\nu) = \int \frac{d^3\vec{p}_{\bar{\nu}}}{(2\pi)^3} f(E_{\bar{\nu}}, \mu_{\bar{\nu}}^*, T) |\vec{v}_\nu - \vec{v}_{\bar{\nu}}| \sigma_{\nu\bar{\nu}\rightarrow Z'}$$

- In a time $\tau_{\nu\bar{\nu}\rightarrow Z'} = c/\langle \mathcal{R}_{\nu\bar{\nu}\rightarrow Z'} \rangle$, $\nu\bar{\nu} \rightarrow Z'$ and Z' decay into $\nu\bar{\nu}$ at a distance $\ell_{Z'}$
- After time t , $\nu\bar{\nu}$ pairs take $N = t/\tau_{\nu\bar{\nu}\rightarrow Z'}$ random steps, which takes them on average a distance $\sqrt{N}\ell_{Z'}$ far away from where they started

For $\sqrt{N}\ell_{Z'} = R_{ns} \Rightarrow$ **the ν diffusion time** $t_{\text{diff}}^{\text{new}} = (R_{ns}/\ell_{Z'})^2 \tau_{\nu\bar{\nu}\rightarrow Z'}$

Describing the proto-NS interior with 6 different shells of radius R_k (different T)

$$t_{\text{diff}}^{\text{new}} = \sum_{k=1}^n \frac{(R_k^2 - R_{k-1}^2)}{(\ell_{Z'}^k)^2} \tau_{\nu\bar{\nu}\rightarrow Z'}^k$$

Total luminosity carried by Z' outside the star

In the regime where $\ell_{Z'} > R_{ns}$, each $\nu\bar{\nu}$ pair producing the Z' on-shell will be transferred outside the neutrinosphere. The energy transfer rate per unit volume and time taken by the Z' can be written as

$$\mathcal{L} = \frac{1}{2\pi^2} \int dE_{\nu\beta} f(E_{\nu\beta}, \mu_{\nu\beta}^*, T) E_{\nu\beta}^2 \int_{E_{\nu\beta}^{min}}^{\infty} 2 \frac{dE_{\bar{\nu}\beta}}{32\pi} f(E_{\bar{\nu}\beta}, \mu_{\bar{\nu}\beta}^*, T) E_{\bar{\nu}\beta} \left(\frac{m_{Z'}}{E_{\bar{\nu}\beta} E_{\nu\beta}} \right)^2 |\overline{\mathcal{M}}|_{\nu\beta\bar{\nu}\beta \rightarrow Z'}^2$$

where the factor 2 at the beginning of the inner integral comes from considering both muon and tau neutrino flavours.

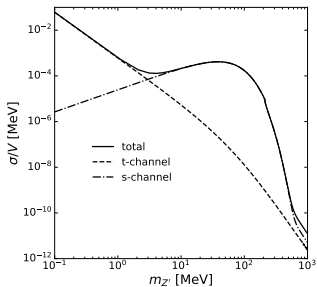
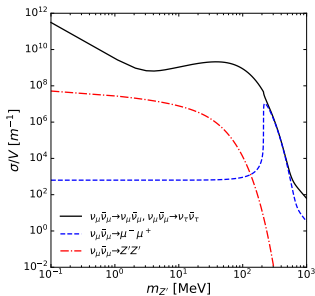
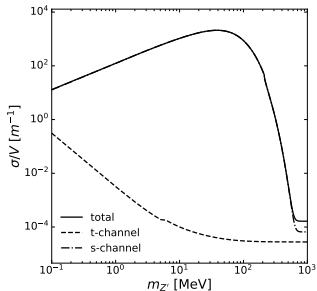
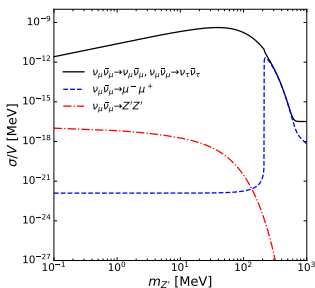
The total energy carried by the Z' per unit time is

$$L = \sum_{k=1}^n \frac{4\pi}{3} (R_k^3 - R_{k-1}^3) \mathcal{L}_k.$$

Imposing $L \leq 3 \times 10^{-52}$ erg/s is equivalent to the upper bound obtained in [Croon et al., JHEP 01 \(2021\) 107](#) for the $U(1)_{L_\mu-L_\tau}$ model. \mathcal{L}_k corresponds to the Z' energy transfer rate per unit volume and time in each shell, which depends on T .

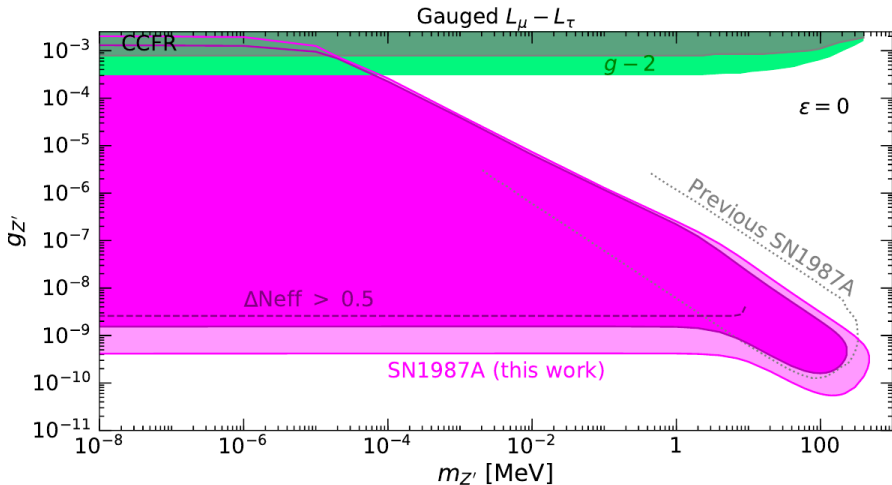
Other interactions and channels

$k = 1$, upper panel $g_{\mu-\tau} = 10^{-4}$, lower panel $g_{\mu-\tau} = 0.1$



Cooling and net muon number effect in the $U(1)_{L_\mu-L_\tau}$

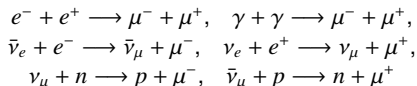
Within the SM, a suppressed population of muons is expected to exist inside a proto-NS. *Croon et al., JHEP 01 (2021) 107* has studied the Z' production by this background muon population through semi-Compton and Bremsstrahlung processes. The effect can be significant only for the Z' masses below ~ 5 MeV.



Muon production in SN in the SM

- The proto-NS may reach $T \sim 50$ MeV before it is cooled by ν diffusion (first 10 s)
- The proto-NS is born with a significant electron to baryon number ratio (from the core of the progenitor star) but no initial muon or tau population
- A net excess of e^- over e^+ occurs due to the high initial electron fraction compensating the positive charge of the protons
- Electrons highly degenerate with a chemical potential $\mu_e > m_\mu$
- The thermal distribution of photons and ν reach well beyond 100 MeV

Under these conditions μ^- and μ^+ are produced via



Net muon population in SN in the SM

- Once core-collapse SN is initiated, e^- and p in the progenitor combine and ν_e quickly diffuse out of the star, decreasing the net lepton number \Rightarrow neutron-rich core
- Due to the excess of e^- over e^+ as well as the one of neutrons over protons, an excess of μ^- over μ^+ is built up
- Due to weak magnetism corrections, the interaction cross section for $N + \nu \rightarrow N + \nu$ is slightly larger than for $N + \bar{\nu} \rightarrow N + \bar{\nu} \Rightarrow \bar{\nu}$ diffuse out of the star faster than $\nu \Rightarrow \mu_\nu \neq 0$
- $\bar{\nu}_\mu$ diffuse out of the star faster than $\nu_\mu \Rightarrow$ net ν_μ population over $\bar{\nu}_\mu$ population \Rightarrow increase of the net μ^- population over μ^+

The process of muonization that leads to an excess of μ^- over μ^+ in the final NS is facilitated by the previous reactions as well as $\nu_\mu + n \rightleftharpoons p + \mu^-$, $\bar{\nu}_\mu + p \rightleftharpoons n + \mu^+$ and

$\nu + \mu^- \rightleftharpoons \nu' + \mu'^-$	$\nu + \mu^+ \rightleftharpoons \nu' + \mu'^+$
$\nu_\mu + e^- \rightleftharpoons \nu_e + \mu^-$	$\bar{\nu}_\mu + e^+ \rightleftharpoons \bar{\nu}_e + \mu^+$
$\nu_\mu + \bar{\nu}_e + e^- \rightleftharpoons \mu^-$	$\bar{\nu}_\mu + \nu_e + e^+ \rightleftharpoons \mu^+$
$\bar{\nu}_e + e^- \rightleftharpoons \bar{\nu}_\mu + \mu^-$	$\nu_e + e^+ \rightleftharpoons \nu_\mu + \mu^+$
$\nu_\mu + n \rightleftharpoons p + \mu^-$	$\bar{\nu}_\mu + p \rightleftharpoons n + \mu^+$

Effect of a net muon number density on the profiles

Negligible effect of the net muon population in the temperature and density profiles *Bollia et al., PRL 125 (2020) 051104*

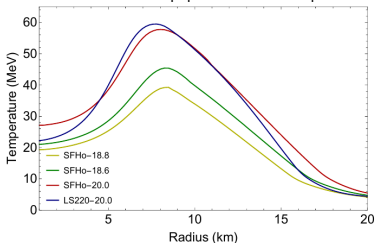


FIG. 1: Temperature profile for various models at 1 s post-bounce.

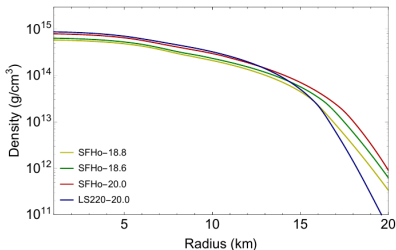


FIG. 2: Density profile for the models corresponding to Fig. 1

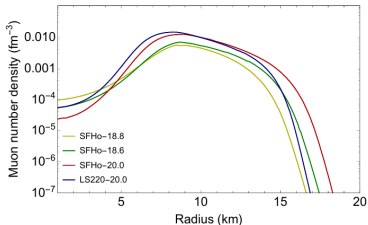


FIG. 3: Muon number density. Note that despite large differences in peak temperature, the muon number density does not change by more than an order of magnitude in the relevant region of high muon density ($5 \text{ km} \lesssim r \lesssim 15 \text{ km}$).

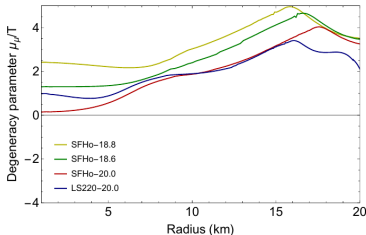


FIG. 4: Muon degeneracy parameter μ_μ/T for various profiles. This ratio never exceeds a small $\mathcal{O}(1)$ value in the relevant region of high muon density ($5 \text{ km} \lesssim r \lesssim 15 \text{ km}$).

Weak magnetism effect on μ_{ν_μ} and μ_{ν_τ}

Horowitz, PRD 65 (2002) 043001

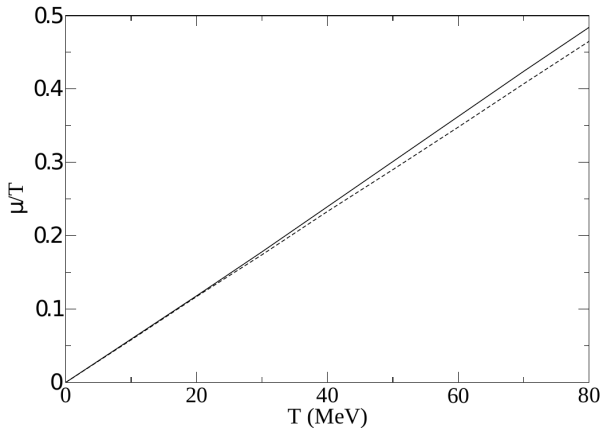


FIG. 3. Muon or Tau neutrino chemical potential over temperature μ_{ν_x}/T versus T for matter in steady state equilibrium. The solid line is the full result from the solution to Eq. (13) while the dashed line is correct to lowest order in k/M and μ/T , Eq. (44)

Reasons to neglect the muon population for our purposes

- The non-negligible amount of muons obtained in *Bollig et al., PRL 125 (2020) 051104* could open a new production mechanism of Z' via muon-photon semi-Compton scattering but it is only relevant for $m_{Z'} < 10$ MeV *Croon et al., JHEP 01 (2021) 107*
- The $Z' + \mu \rightarrow \mu + \gamma$ mean free path is ~ 60 km $(7 \times 10^{-8} / g_{\mu-\tau})^2$, which for $m_{Z'} > 10$ MeV is larger than the decay length of Z' by more than one order of magnitude \Rightarrow the Z' decays long before undergoing any scattering
- For $m_{Z'} \geq 211.3$ MeV the $\nu\bar{\nu}$ annihilation into muons via s -channel Z' diagram is possible, but these processes generate the same amount of muons and antimuons $\Rightarrow \mu_{\mu^-} = \mu_{\mu^+} = 0$ (as we assume in the SM) and therefore we do not expect the equation of state of the nuclear matter to change
- ν_{μ} ($\bar{\nu}_{\mu}$) can scatter on μ^+ (μ^-), but $n_{\mu} \ll n_n$ and $\sigma_{\nu_{\mu},\mu} \ll \sigma_{\nu_{\mu},n}$, the mean free path of scattering on μ^- (μ^+) is negligible compared to the scattering on n

Effect of the production of muons by new physics

- Will $\nu\bar{\nu}$ annihilation into muons via s -channel Z' diagram have an impact on the physics of the proto-NS?
- These processes generate the same amount of muons and antimuons \Rightarrow
 $\mu_{\mu^-} = \mu_{\mu^+} = 0$ (as we assume in the SM) and therefore we do not expect the equation of state of the nuclear matter to change
- ν_{μ} ($\bar{\nu}_{\mu}$) can scatter on μ^+ (μ^-), but $n_{\mu} \ll n_n$ and $\sigma_{\nu_{\mu},\mu} \ll \sigma_{\nu_{\mu},n}$, the mean free path of scattering on μ^- (μ^+) is negligible compared to the scattering on n
- The decay of muons into muon neutrinos close to the neutrinosphere can change equality between the muon neutrino and tau neutrino fluxes that come out of the neutrinosphere, having consequences for collective neutrino oscillation

Supernova bounds on new neutrino physics

Farzan et al., *JHEP* 05 (2018) 066, Suliga, Tamborra, *PRD* 103 (2021) 083002 derived bounds on ν -N interactions in models with light scalar and vector mediators imposing $t_E \lesssim 10$ s

Cerdeño, Cermeño, Pérez-García and Reid, *PRD* 104 (2021) 063013 improved these bounds taking into account the temperature, T , and density, n_B , effects on the ν mean free path, λ_ν

m_N^* effective nucleon mass,

$\mu_{\nu_e}^*, \mu_n^*, \mu_p^*$,

ν_e , neutron (n), proton (p)

effective chemical potentials,

$\mu_{\nu_\mu} = \mu_{\nu_\tau} = 0$

$$f(E_j, \mu_j^*, T) = \frac{1}{1 + e^{(E_j - \mu_j^*)/T}},$$

distribution function of the target,

$j \equiv N = n, p$

T, n_B and Y_e from Fischer et al., *PRD* 85 (2012) 083003

	R (km)	T (MeV)	n_B (fm $^{-3}$)	Y_e	μ_n^* (MeV)	μ_p^* (MeV)	$\mu_{\nu_e}^*$ (MeV)	m_N^* (MeV)
$k = 1$	5.0	15	0.5	0.3	496.6	405.4	114.6	249.6
$k = 2$	7.5	20	0.3	0.28	530.0	458.3	102.7	384.9
$k = 3$	10.0	28	0.15	0.25	656.5	601.9	79.9	599.4
$k = 4$	15.0	33	0.06	0.2	779.8	723.0	29.0	786.0
$k = 5$	17.5	18	0.03	0.1	858.7	813.1	14.4	857.0
$k = 6$	20.0	7	0.008	0.05	917.2	893.9	12.5	915.9

$$c \Delta t \equiv c t_{\text{diff}} = \sum_{k=1}^n \left(R_k^2 - R_{k-1}^2 \right) \langle 1/\lambda_\nu \rangle_k, \quad \langle 1/\lambda_\nu \rangle = \frac{\int dE_\nu f(E_\nu, \mu_\nu^*, T) E_\nu^2 \lambda_\nu^{-1}(E_\nu)}{\int dE_\nu f(E_\nu, \mu_\nu^*, T) E_\nu^2}$$

$$\lambda_\nu^{-1}(E_\nu) = \sum_j \int g_j \frac{d^3 \vec{p}'_j}{(2\pi)^3} f(E_j, \mu_j^*, T) \int \frac{d^3 \vec{p}'_\nu}{(2\pi)^3 2E'_\nu} \int \frac{d^3 \vec{p}'_j}{(2\pi)^3 2E'_j} (2\pi)^4 \delta^{(4)}(p_\nu + p_j - p'_\nu + p'_j) \frac{|\overline{\mathcal{M}}_{\nu j}^2}{4E_\nu E_j} (1 - f(E'_\nu, \mu_\nu^*, T))(1 - f(E'_j, \mu_j^*, T))$$

Bounds on new ν -N interactions from the ν diffusion time in the SN interior

Cerdeño, **Cermeño**, Pérez-García and Reid, PRD 104 (2021) 063013

$$\Delta t \lesssim 2 \Delta t^{\text{SM}}, \quad \Delta t^{\text{SM}} \sim 1 \text{ s}$$

Δt includes both new physics and SM interactions, i.e., the $2 \Delta t^{\text{SM}}$ line indicates where new physics interactions starts contributing equally to the diffusion time than SM interactions

$$\mathcal{L}_{\text{LNC}} \supset -C_V \bar{\nu}_R \phi \nu_L - \bar{\psi}_N C_N \psi_N \phi - \sum_l C_l \bar{l} \phi l,$$

$$Y = \sqrt{C_V C_N}$$

$$\mathcal{L}_{\text{B-L}} = -\sum_q C_q \bar{q} \gamma^\mu q Z'_\mu - \sum_l C_l \bar{l} \gamma^\mu l Z'_\mu - \sum_\nu C_\nu \bar{\nu} \gamma^\mu \nu Z'_\mu$$

$$C_q = g_{\text{B-L}}/3, C_{l,\nu} = -g_{\text{B-L}}$$

